Characterization of Single-Mode Fibers from Wavelength Dependence of Modal Field and Far Field

ANTONIO C. CAMPOS, RAMAKANT SRIVASTAVA, AND J. A. ROVERSI

Abstract—We present direct methods for determination of equivalent-step-index (ESI) parameters and the modal field by measurement of the wavelength dependence of the far-field intensity in single-mode fibers. A comparison is made with the spot-size method commonly used for characterization of such fibers. A new technique for measuring the LP_{11} mode cutoff wavelength is also presented.

I. Introduction

CHARACTERIZATION of single-mode fibers has attracted a great deal of attention in the recent past. When the fiber has a step-index profile, the two parameters of interest are the relative index difference Δ and the core radius a. However, in practice it is difficult to fabricate ideally step-index fibers and the concept of equivalent-step-index (ESI) fibers has been invoked [1], wherein the modal field of the real fiber with arbitrary index profile is the same as that for the ESI fiber. The concept is originally based on the approximation that the modal field of any single-mode fiber is Gaussian. Thus the process of characterization of a single-mode fiber of arbitrary index profile reduces to determination of the equivalent core radius a_s and the equivalent Δ-value Δ_s, or the normalized frequency v_s or the cutoff wavelength λ_c of the LP_{11} mode.

The first determination of v_s and a_s was made by Gambling *et al.* [2] in 1976 when they measured the far-field intensity distribution of a single-mode fiber and determined the angles corresponding to half the maximum intensity (θ_h) and the first minimum (θ_x). Since the theory assumed a step-index profile, using a set of two universal curves, the authors determined the v_s and a_s values. Later, Pask and Sammut [3] suggested that if the same analysis were extended to graded-index fibers, one would obtain the ESI parameters. The validity of this extension was demonstrated recently by comparing the spot-size of a fiber derived from its far field to that obtained from the near field [4]. However, the technique of [2] and [3] suffers from a great disadvantage—the intensity of the first minimum lies 40–70 dB below the central maximum and it is not always easy to detect its presence. Moreover, in the present day single-mode fibers, the interest lies in the 1.2–1.6-μm region, where due to lack of good detectors, a large dynamic response is even more difficult to achieve. This is probably why the technique was not pursued further.

In this work, we have revisited the method and demonstrated that the two ESI parameters a_s and v_s can be obtained directly by fitting the far-field data to the theoretical expression for the pattern [2], eliminating thereby the necessity to measure the angle of the first minimum (θ_x) and making use of all the data points instead of only θ_h and θ_x values. Furthermore, the core radius a_s has been obtained with high accuracy by averaging its value for different wavelengths. Moreover, since $v_s = (2\pi/\lambda)a_s\,(\mathrm{NA})_s$, we obtain the effective numerical aperture to a high accuracy by fitting the $v_s(\lambda)$ curve to a straight line. We have also extended our analysis to test the validity of the suggestion recently made by Pask and Rühl [5] in which the wavelength dependence of the half-intensity angle θ_h should be measured and fitted to an empirical relation to yield the effective core radius a_s and the LP_{11} mode cutoff wavelength λ_c.

In an attempt to compare the ESI parameters as obtained from the far field using the analysis outlined above, we have also resorted to the popular approach [6] in which modal width ω is measured as a function of wavelength λ. Although many variations of this approach have been reported so far [6]-[9], the most accepted one fits the $\omega(\lambda)$ curve to the empirical relation given by Marcuse [10], yielding thereby the values of a_s and λ_c. We show in this work that the value of λ_c obtained from the $\omega(\lambda)$ curve is very sensitive to external perturbations and can give unreliable results if due care is not taken. Here we suggest a simple, direct, independent, and accurate method to determine λ_c and obtain the values of the effective core-radius to a better accuracy.

Finally, we present a direct technique for determination of the Gaussian-exponential modal field starting from the measured far field. It is based on a recent work [4] in which it was shown how the measurement of θ_h and θ_x can yield the two parameters of the Gaussian-exponential modal field. In order to eliminate the need to measure θ_x, we have again fitted all the data points to the theoretical expression of [4] to obtain the modal-field parameters directly. Some comments are also made about the adequacy of the Gaussian-exponential approximation.

II. Techniques

The far-field intensity distribution for a step-index single-

Manuscript received February 8, 1984. This work was supported by Telebras S/A. A. C. Campos received a graduate fellowship from FAPESP and Sociedade Cultural e Beneficente Guilherme Guinle.

The authors are with Instituto de Física, UNICAMP, Campinas, SP 13.100 Brazil.

0733-8724/84/0800-0334$01.00

mode fiber has been given by Gambling *et al.* [2]

$$|\Psi|^2 = \left| \frac{u^2 w^2}{(u^2 - \alpha^2)(w^2 + \alpha^2)} \left\{ J_0(\alpha) - \alpha J_1(\alpha) \frac{J_0(u)}{u J_1(u)} \right\} \right|^2, \quad \text{for } u \neq \alpha \quad (1)$$

$$= \left| \frac{u^2 w^2}{2v^2} \frac{1}{u J_1(u)} \{ J_0^2(\alpha) + J_1^2(\alpha) \} \right|^2, \quad \text{for } u = \alpha$$

where $\alpha = ka \sin \theta$ and u, v, and w are the well-known parameters [11]. If one used an analytical expression which relates u and v for the fundamental mode then the expression (1) is a function of only two variables v and a. We have found that the empirical relation

$$u = \frac{(1 + \sqrt{2})\, v}{|1 + (4 + v^4)^{1/4}|}$$

given by Gloge [11] is reasonably satisfactory compared to the exact relation. Using (2) in (1), we have fitted the experimental data and derived the values of v and a at various wavelengths in the single-mode region. Since a is expected to be wavelength independent, the λ-dependence of the v-value gives the effective numerical aperture. In order to accurately determine this parameter, we chose to do least-square fitting of the v versus λ^{-1} curve to a straight line and obtain the Δ_s value from the slope of the line.

Alternatively, it has recently been suggested [5] that the two universal curves derived by Gambling *et al.* [2] from (1) can be accurately represented by an empirical relation

$$k a_s \sin \theta_h = 2.3216 - 1.7426 (\lambda/\lambda_c) + 0.3563 (\lambda/\lambda_c)^2, \quad \text{for } 0.75 \leqslant \lambda/\lambda_c \leqslant 1.5. \quad (3)$$

Thus the wavelength dependence of the half-intensity angle θ_h can be fitted to (3) to give a_s and λ_c. It must however be pointed out that θ_h varies very little with the wavelength, and a high accuracy in its measurement is called for in order to exploit (3) for fiber characterization. We have found that θ_h can be determined satisfactorily by using a Gaussian fit to the far-field data over the range of angles where the far-field-intensity profile does not deviate from Gaussian [12]. We have noticed that this is easily satisfied for the derived v-values provided we consider only those data points for which

$$I(\theta) \leqslant \frac{I(\theta = 0)}{10}.$$

On the other hand, if we assume that the modal field of a single-mode fiber is Gaussian, independent of the refractive-index profile, then the field can be described by only one parameter called the modal width or the spot size ω whose wavelength dependence gives the ESI parameters [1]. We have measured the spot size as a function of wavelength using the splice-loss technique [6]. For the source of radiation, both a white-light lamp and a fiber Raman laser were used, and since the latter gave more accurate values due to higher signals detected, all the data reported here correspond to this source. Once the $\omega(\lambda)$ curve was obtained, the next problem was to define the method of deriving the ESI parameters. In recent years, many different methods have been suggested in the literature and it has also been pointed out [7] that each one gives different results. We have confined our analysis to two conventional methods and have introduced a new method which seems to give better results. In the first method, the cutoff wavelength λ_c was defined as the point of intersection of straight lines which are tangents to the $\omega(\lambda)$ curve on both sides of the LP_{11} mode cutoff. This is basically Millar's method [6] and we have utilized his equations to give Δ_s and a_s. In the second method, we followed the suggestion of Allard *et al.* [8] and fitted the $\omega(\lambda)$ curve in the region $\lambda > \lambda_c$ to the empirical relation given by Marcuse [10] and rewritten by Allard *et al.* [8]

$$\omega = a_s \left| 0.65 + 0.434 \left(\frac{\lambda}{\lambda_c} \right)^{3/2} + 0.0149 \left(\frac{\lambda}{\lambda_c} \right)^6 \right| \quad (4)$$

to give the values of a_s and λ_c.

Although the merits of the new method proposed by us will be discussed later, we would outline the basic procedure here. During the curve fitting procedure using a Gaussian for the transmission-loss curve, whenever the LP_{11} mode was present, two symmetrically located shoulders were detected. We noticed that the detection of this symmetrical deviation from a Gaussian was sensitive to the wavelength and we could measure the cutoff wavelength with great precision. This value was then used in (4) to obtain the a_s-value.

Although Gaussian approximation to the modal field has been used widely for the simplicity it offers in calculations of the propagation characteristics of single-mode fibers, it is well known that it is not an accurate description for v-values of practical interest [13]. For such fibers, the field has been shown to be better described by a Gaussian-exponential [14]

$$E(r) = A e^{-(r/b)^2}, \quad r < d$$
$$= A e^{-d(2r-d)/b^2}, \quad r > d. \quad (5)$$

The resultant far-field distribution can be written as [4]

$$I(\theta) = I(0) \frac{16\eta^4}{(2\eta + e^{-\eta})^2} \left| \frac{2\eta e^{\eta}}{(4\eta^2 + \epsilon^2)^{3/2}} + \int_0^1 J_0(x\epsilon)(e^{-\eta x^2} - e^{-\eta(2x-1)})\, x\, dx \right|^2 \quad (6)$$

where $\eta = (d/b)^2$ and $\epsilon = kd \sin \theta$.

We have fitted our data to the preciously mentioned expression and obtained the two parameters d and b directly, without the need of determining the angles θ_h and θ_x used earlier [4]. Following the determination of d and b for each wavelength, we calculated the spot-size values as pointed out in [4] and compared them with those obtained from Millar's technique [6].

III. Experimental

Four different fibers were measured. The nominal values of the parameters for each fiber as given by the manufacturer are shown in Table I.

Due to lack of an adequate source in the visible region, we did not measure the wavelength dependence of parameters in the case of fiber D. We have also not measured the $\omega(\lambda)$ curve

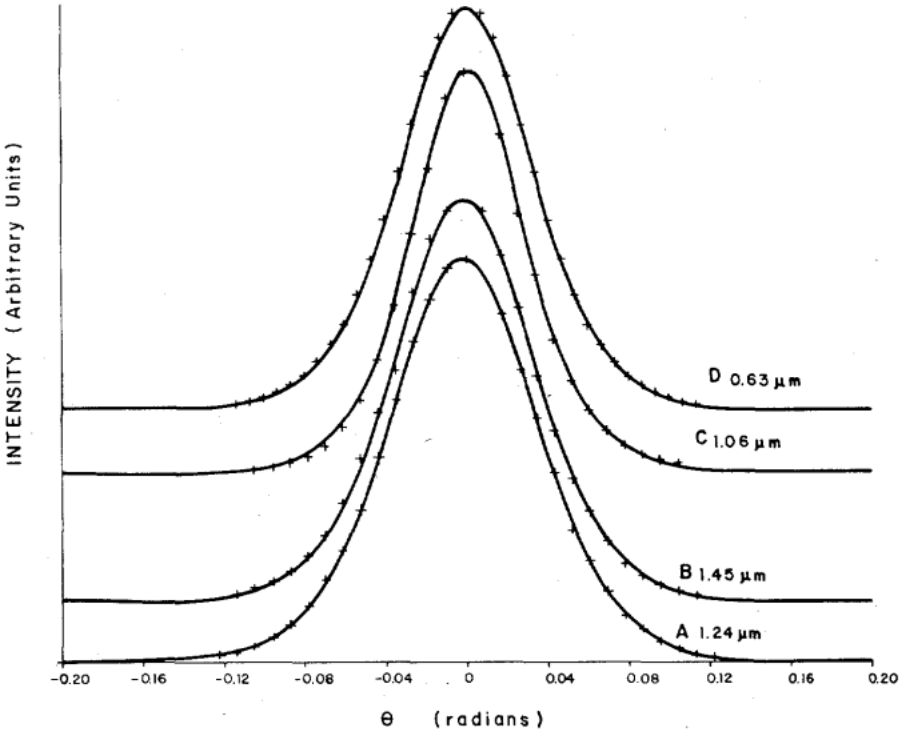

Fig. 1. Far-field intensity distribution of fibers A, B, C, and D at the wavelengths indicated. The continuous curves have been obtained by fitting the data to (1). The curves have been displaced vertically for clarity.

TABLE I

Fiber	N.A.	λ_c (μm)	2a (μm)	Profile
A	0.1	1.2	~10	~ step with central dip
B	0.1	1.3	~10	~ step with central dip
C	0.2	0.9	8	triangular
D	0.1	0.5	~5	~ step with central dip

for fiber C, although we know a priori from its far field that the near field is expected to be far from a Gaussian. Experiments were carried out at 6328 Å, in the case of fiber D and in the 1.06–1.50-μm region in the other three fibers. In the case of fiber D, we could measure θ_x also, because a high sensitivity photomultiplier provided the large dynamical range needed. Far-field measurements were generally made by fixing the detector position and rotating the fiber-exit end. However, in the case of fiber D, we fixed the fiber end and scanned the photomultiplier position. Special precautions [15] were taken to mask any stray light in this case. When the fiber Raman laser was used as the source, we launched light directly from the Raman fiber into the test fiber and the wavelength selection was made at the exit end of the test fiber. This facilitates the setup and the coupling conditions to the fiber remain steady during wavelength scanning. Care was taken to avoid nonlinear effects in the test fiber. To prevent this from occurring, the test fiber end had to be kept at a minimum distance of 2 mm from the Raman fiber end. The signal averaging was done by either using a box car or a lock-in amplifier. Far-field data were taken point by point and in general 25–30 data points were collected for each wavelength.

For measurement of the $\omega(\lambda)$ curve, the donor part of the test fiber was mounted in front of the Raman fiber and the acceptor part on a motorized translation device to provide steps of 0.4 μm each. The transmission loss curve was also obtained point by point for each wavelength and ω was determined by a least-square fit to a Gaussian. The reproducibility in the measurement of ω was checked by making at least ten measurements for each λ. The values used in the analysis are averages of these separate measurements and are highly accurate, estimated to have an error of less than 1 percent.

IV. Results

A. ESI Parameters from the Far-Field Pattern

Fig. 1 shows the far-field intensity patterns for the fibers measured. The wavelengths are specified for each case and the fitting to (1) is shown by the continuous curves. It may be observed that the fitting is very good in each case. The wavelength dependences of the parameters v_s and a_s, for fibers A, B, and C, are shown in Fig. 2. As expected, a_s is reasonably invariant and v_s is inversely proportional to the wavelength. Using the average value of a_s, we have determined Δ_s from the slope of the $v_s(\lambda)$ line. These ESI parameters are shown in Table II for each fiber. In the case of fiber D, the two parameters v_s and a_s, obtained by fitting the far-field pattern to (1) at 6328 Å were found to be in good agreement with those obtained by using universal curves [2], [3]. In this case, therefore, the values shown in Table II are those obtained from this set.

Fig. 3 shows the dependence of θ_h on wavelength for three fibers. The continuous curves are least-square fits to the data

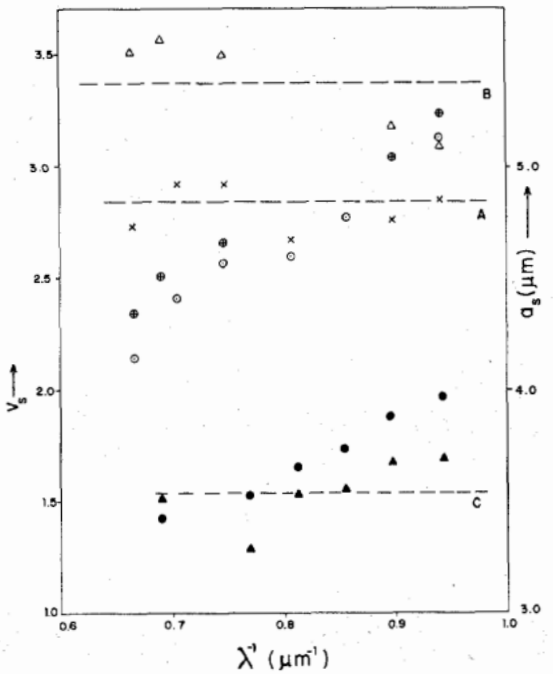

Fig. 2. Wavelength dependence of the ESI parameters v_S and a_S; ⊙, ⊕, and ● denote v_S values for fibers A, B, and C, respectively; ×, Δ, and ▲ are the respective a_S values and the dashed lines are their averages.

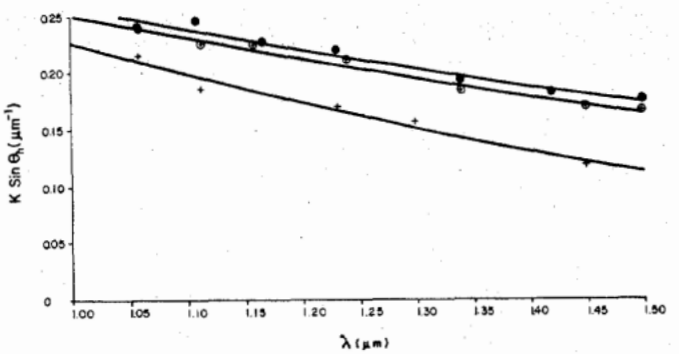

Fig. 3. Far-field intensity half angle θ_h of equivalent-step-index fiber as a function of wavelength. The curve is the least-square fit to the data using (3). ⊕ fiber A, ● fiber B, and + fiber C. The ESI parameters are given in Table II.

TABLE II

Fiber	Expression (1)			Expression (3)		
	a_s	Δ_s	λ_c	a_s	Δ_s	λ_c
A	4.84	2.6×10^{-3}	1.33	4.75	2.6×10^{-3}	1.30
B	5.37	2.1×10^{-3}	1.33	4.75	2.8×10^{-3}	1.35
C	3.54	2.4×10^{-3}	0.93	3.77	2.1×10^{-3}	0.92
D	1.88	2.5×10^{-3}	0.51	-	-	-

using (3). The values of the parameters a_s and λ_c, obtained by fitting, are given in Table II. As can be seen, the fitting is not very good. There may be three reasons for this to occur. Firstly, the technique to get θ_h is not ideal and suffers from the error of assuming a Gaussian. Secondly, the variation of θ_h with λ in the wavelength range studied is very little. And finally, we believe a large number of data points in the far field

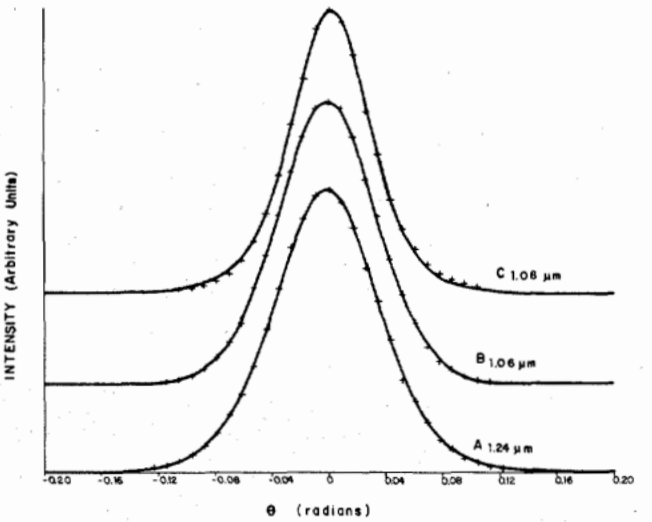

Fig. 4. Far-field intensity data fitted to the expression (6) derived from a Gaussian-exponential modal field. The wavelengths are specified next to the respective curves. The curves have been displaced vertically for clarity. The fitted parameters are given in Table III.

TABLE III

Fiber	λ (μm)	Gaussian-Exponential			Gaussian
		d (μm)	b (μm)	ω (μm)	ω (μm)
A	1.24	5.38	4.71	4.71	5.32
	1.34	6.32	5.24	5.24	5.63
B	1.14	6.27	4.82	4.82	5.87
	1.34	6.07	5.39	5.39	5.75
	1.50	5.46	5.64	5.64	6.28
C	1.06	2.54	3.65	3.89	-
	1.114	2.27	3.56	3.93	-
D	0.633	2.15	2.33	2.38	2.64

at a larger number of wavelengths would be desirable to improve the accuracy, needing thereby an automated data acquisition and analysis system.

B. Determination of the Gaussian-Exponential Modal Field from Far Field

Fig. 4 shows the far-field data fitted to the expression (6) for three fibers at the wavelengths specified. It was observed that although in the case of fibers A and B, the fit was very good at all the wavelengths studied, the same was not true for fiber C—the fitting gave unphysical values for the parameters at wavelengths higher than 1.1 μm corresponding to the v_s-values lower than 2.0. This limitation will be discussed later in Section V. Table III gives the values of the parameters d and b obtained from the fit. In the case of fiber D, the values are the same as obtained from the use of universal curves [4], supporting the validity of the fitting procedure. Next, the spot size was determined from the expression given in [4] and in Table III we have given these values at the wavelengths studied for each fiber.

C. Gaussian Modal Field and Spot Size

Fig. 5 shows $\omega(\lambda)$ curves for fibers A and B. ω was determined by fitting a Gaussian to the transmission-loss curve of

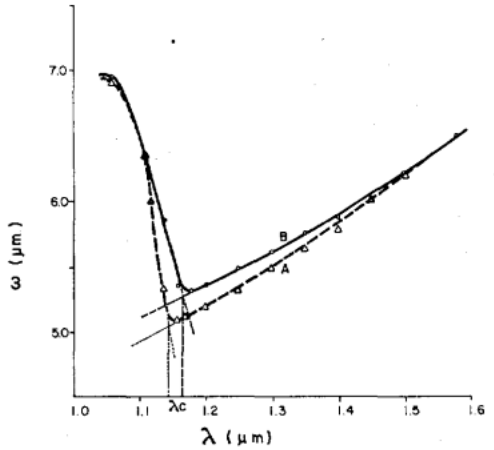

Fig. 5. Spot-size dependence on wavelength for fibers *A* and *B*.

TABLE IV

Fiber	Millar's Method			Allard's Method			Our Method		
	a_s (μm)	λ_c (μm)	Δ_s	a_s (μm)	λ_c (μm)	Δ_s	a_s (μm)	λ_c (μm)	Δ_s
A	4.60	1.15	2.2×10^{-3}	4.76	1.21	2.2×10^{-3}	4.73	1.20	2.2×10^{-3}
B	4.82	1.17	2.1×10^{-3}	5.24	1.34	2.3×10^{-3}	5.01	1.25	2.2×10^{-3}

the splice [10] using cladding mode strippers. It was observed that the transmission-loss curve fitted very well to the Gaussian only in the region above the cutoff wavelength ($\lambda > \lambda_c$). For $\lambda < \lambda_c$, the data presents symmetrical deviations from the Gaussian in the form of two shoulders on each side of the central peak, reminiscent of the presence of the LP_{11} mode. The presence of the LP_{11} mode is, however, subject to the external perturbations [16] and the fiber length. When fibers with large lengths (~100 m) were used, there was no trace of this mode in the $\omega(\lambda)$ curve in our studies. It must be pointed out, however, that although the value of the spot size determined by the fitting procedure does not necessarily reflect the transition to dual-mode operation and is relatively insensitive to the onset of the higher order mode, the observation of the symmetric shoulders referred to earlier in the fitting can be easily monitored to determine the cutoff wavelength λ_c with great precision. These values of λ_c are shown in Table IV.

As has been pointed out earlier, in order to determine the ESI parameters from the $\omega(\lambda)$ curve, we have used three different procedures. First we evaluated λ_c by extrapolation of the tangents on both sides of the point of inflexion according to the suggestion of Millar [6]. Next, the values of a_s and Δ_s were determined by the procedure outlined in [6]. These parameters are given in Table IV. In the second procedure, we fitted the $\omega(\lambda)$ curve in the region $\lambda > \lambda_c$ to the empirical expression given by Marcuse (4) in this paper. This procedure gives the values of a_s and λ_c shown in the same Table IV. Finally, we have used the value of λ_c as determined by the Gaussian fitting procedure outlined in the previous paragraph to obtain the value of the equivalent core-radius using (4). The values of a_s thus obtained are also given in Table IV.

V. Discussion

A. Spot-Size Data Analysis

In order to analyze the results given in Tables II–IV, we will first concentrate on Table IV which gives the ESI parameters obtained from the $\omega(\lambda)$ curve. As has been pointed out extensively in the literature [8], [16], [17], we verify that Millar's method underestimates the value of λ_c and consequently that of a_s. This occurs due to the inevitable presence of microbending losses introduced in the fiber during handling and mounting the experiment. The errors in λ_c caused by microbending have been reported to be as high as 100 nm [17]. A theoretical analysis of the effects of loss in equivalent step-index single-mode fibers has recently been reported by Pask and Rühl [16] confirming these observations. In order to further test the meaningfulness of the ESI parameters in the case of fiber *A*, and to confirm their underestimation in Millar's method, we carried out calculations of the profile dispersion using these parameters. Although, the justification for the use of the ESI parameters in estimating the waveguide dispersion has been subject to debate in the literature [18]–[21], we were encouraged to use them due to their relative success reported recently [20] and verified by us [22]. Moreover, the objective was to get only a qualitative estimate of the effect of the waveguide and not a quantitative analysis. Assuming that the material and profile dispersion are additive and the core and cladding have the same dispersive properties, results showed that the wavelength of the zero material dispersion in fiber *A* was much below that of pure silica if the set of parameters derived by Millar's method are used.

In regard to the acceptability of the ESI parameters given by the fitting procedure of Allard *et al.* [8], it has been pointed out [16] that (4) can be made to fit the spot-size data reasonably well even if both λ_c and a_s are given incorrect values. Yet, the procedure yields substantially correct numerical aperture. However, if the cutoff wavelength is determined independently and fed into (4), the value of the core radius will come out to be very accurate. This led us to establish some other procedure for determining λ_c. As has been discussed earlier, in Section IV, in the process of fitting a Gaussian to the splice-loss transmission data the presence of the LP_{11} mode could be observed by the symmetrical deviation of the data from the Gaussian around the perfectly aligned fiber position. This occurred in form of two humps as would be expected from the contribution of the LP_{11} mode which would be better excited at offset positions. We found that as the wavelength approached the cutoff value from below, the deviation became smaller and smaller until it became undetectable in the single-mode region. It must be emphasized however, that this was feasible only because we had a very high signal-to-noise ratio in our data, due to the fact that a Raman laser was used as the source. The value of λ_c thus measured was then used to obtain a_s from (4). The results are shown in Table IV (our method). Although in the case of fiber *A*, the difference between the two sets of parameters (our method and Allard's method) is negligible, in fiber *B* it is substantial. The relative insensibility of Δ_s to the values of a_s and λ_c is also observed. We believe that although the technique for determination of λ_c described here is very

sensitive and can be used without necessity of any excess work because the Gaussian fitting procedure for the determination of spot size is a necessary step anyway, more work needs to be carried out to show its superiority. We must add here that both the sets of parameters obtained by fitting (4) to the spot-size data are acceptable from the point of view of predicting waveguide dispersion to a reasonable degree [22].

B. Far-Field Data Analysis

1) ESI Parameters: An analysis of Table II and its comparison with the last set of values given in Table IV shows that the far-field data gives a larger value of λ_c no matter which of the two expressions (1) or (3) is used to extract its value. The λ_c-value obtained from the far-field data is also independent of length, unlike the case of spot-size method. This makes us believe that the far-field technique for measurement of the cutoff wavelength gives the theoretical value which is always higher than the real value. Although it has been argued that a system designer is least interested in the theoretical value, more work needs to be done to define the cutoff wavelength to be used for single-mode fiber specifications. The values of core-radii as predicted by the far-field technique are higher if expression (1) is used whereas there is no defined trend in the case of (3). We believe that the discrepancies in the results using (3) can be substantially eliminated if a better method for determining θ_h is employed. In principle, the two expressions offer the same potential and one would expect to obtain the same values for the ESI parameters. But owing to the lack of precise data, shown in the fitting in Fig. 3, we have not been able to drawn any firm conclusions. Moreover, we believe that more fibers have to be measured in order to make any conclusive remarks.

A few words must be said here about the possible reasons for the discrepancies in the values of the ESI parameters obtained by the far-field data and the spot-size data. While the first uses exact expression for the field, the spot-size data is always analyzed assuming that the modal field is Gaussian. It has been shown that although the Gaussian approximation works reasonably well near the cutoff wavelength for most fibers of practical interest, it is unsatisfactory at lower v-values. Since the spot-size data is normally measured up to wavelengths corresponding to v-values of 2.0 or lower, an analysis based on the Gaussian modal field is likely to introduce errors in the ESI parameters. The same is not however true for the far-field analysis where (1) describes the data accurately as has been demonstrated in the curve fittings shown in Fig. 1 for various fibers. We have observed that in the case of fiber *C* (triangular profile) for v-values as low as 1.4, there is no noticeable deviation of the data from the theoretical expression (1).

2) Gaussian-Exponential Modal Field: Finally, we have tested the predictions about the behavior of the spot size as a function of wavelength assuming that the modal field is better described by a Gaussian exponential [14]. The recent success [4] in determining the two modal-field parameters from the far-field measurements induced us to verify their wavelength dependence and the prediction of the spot-size behavior. The last two columns of Table III compare the values of the Gaussian-exponential field spot sizes with those obtained by Millar's method [6] for few wavelengths. As can be observed, the first column values are 10–20 percent lower than those given in the latter. Moreover, their wavelength dependence is also substantially different. This fact, added to the observation made earlier in Section IV that in the case of fiber *C* it was not possible to fit the far-field data by the Gaussian exponential given by (6) and obtain physically meaningful parameters for wavelengths above 1.114 μm, leads us to believe that the behavior of the modal field may not be well described by (5). Recent failure in the attempts to predict the waveguide dispersion using this kind of modal field has also indicated [23] that (5) may not be suitable description of the modal field. It has been suggested that although the field is close to Gaussian up to a certain point across the core, its behavior further away may instead be better described by the Hankel function and not by an exponential [23]. Further work needs to be carried out to test these assumptions.

VI. Conclusion

We propose new methods and improvements in the existing techniques for determination of the ESI parameters of single-mode fibers. It has been shown that if the measured wavelength dependence of the far-field intensity profile is fitted to the theoretical expression for a step-index fiber directly, then the results give the ESI parameters with the LP_{11} mode cutoff wavelength and the core-radius values slightly higher than obtained by the spot-size method. The advantages of the methods include:

1) independence of the length of the fiber measured;
2) technique of far-field measurement is easy to carry out and does not need careful and special end-preparation and characterization technique;
3) eliminates need to measure the intensity points corresponding the first minimum, and
4) theory used is exact and does not need the Gaussian approximation for the modal field as used in the spot-size method.

Our analysis also shows that the recently suggested method proposed by Pask and Rühl [5] has the same potential provided θ_h is measured with the desired precision. Our attempts on two fibers show inconclusive results about the practical utility of the method.

It is also shown that the wavelength dependence of the two-parameter Gaussian-exponential modal field does not predict right behavior for the spot sizes. Moreover, for v-values below certain value the far-field data yields unrealistic modal field showing the inadequacy of the theory of [14].

Finally, we present a new method for an accurate determination of the LP_{11} mode cutoff from the splice-loss transmission measurements as a function of wavelength. The method proposed is sensitive to the onset of the higher order mode. The value of the effective core radius is then obtained by using the Marcuse formula [10]. It is also shown that Millar's procedure of deriving the ESI parameters from the spot-size data is subject to fiber loss conditions and underestimates the cutoff wavelength and the core radius.

ACKNOWLEDGMENT

The authors wish to thank Furukawa, Fujikura, and BTRL for their donation of the fibers used in this research.

REFERENCES

[1] H. Matsumura and T. Suganuma, *Appl. Opt.*, vol. 19, p. 3151, 1980.
[2] W. A. Gambling, D. N. Payne, H. Matsumura, and R. B. Dyott, *IEE J. Microwaves, Opt. & Acoust.*, vol. 1, p. 13, 1976.
[3] C. Pask and R. A. Sammut, *Electron. Lett.*, vol. 16, p. 310, 1980.
[4] A. K. Ghatak, R. Srivastava, I. F. Faria, K. Thyagarajan, and R. Tiwari, *Electron. Lett.*, vol. 19, p. 97, 1983.
[5] C. Pask and F. Rühl, *Electron. Lett.*, vol. 19, p. 658, 1983.
[6] C. A. Millar, *Electron. Lett.*, vol. 17, p. 458, 1981.
[7] M. Fox, in *Tech. Dig., Symp. Opt. Fiber Measurements* (Boulder, CO), 1982.
[8] F. Allard, L. Jeunhomme, and P. Sansonetti, *Electron. Lett.*, vol. 17, p. 958, 1981.
[9] J. P. Pocholle, J. Auge, J. Raffy, M. Turpin, and M. Papuchon, in *IOOC'83 Tech. Dig.* (Tokyo, Japan), June 1983.
[10] D. Marcuse, *Bell Syst. Tech. J.*, vol. 56, p. 703, 1977.
[11] D. Gloge, *Appl. Opt.*, vol. 10, p. 2252, 1971.
[12] E. Nicholaisen and P. Danielsen, *Electron. Lett.*, vol. 19, p. 28, 1983.
[13] R. Srivastava, A. C. Campos, and J. A. Roversi, presented at Opt. Fibers Conf. '84, New Orleans, LA, Jan. 1984.
[14] R. Tiwari, K. Thyagarajan, B. P. Pal, and A. K. Ghatak, *Opt. Commun.*, vol. 44, p. 94, 1982.
[15] K. Hotate and T. Okoshi, *Appl. Opt.*, vol. 18, p. 3265, 1979.
[16] C. Pask and F. Rühl, *Electron. Lett.*, vol. 19, p. 643, 1983.
[17] P. D. Nichols, *Electron. Lett.*, vol. 18, p. 1008, 1982.
[18] B. P. Nelson and S. Hornung, *Electron. Lett.*, vol. 18, p. 272, 1982.
[19] C. A. Millar, in *Opt. Fiber Commun. '82* (Phoenix, AZ), paper ThEE2.
[20] P. Sansonetti, *Electron. Lett.*, vol. 18, p. 138, 1982.
[21] V. A. Bhagavatulla, *Electron. Lett.*, vol. 18, p. 319, 1982.
[22] A. C. Campos and R. Srivastava, to be published.
[23] I. C. Goyal, private communication.

*

Antonio C. Campos, photograph and biography not available at time of publication.

*

Ramakant Srivastava, biography and photograph not available at time of publication.

*

J. A. Roversi, biography and photograph not available at time of publication.